The Journal of the Acoustical Society of America

SEPTEMBER 09 2026

Comparing measured sonic boom turbulence-induced variability with computational models for the Carpet Determination in Entirety Measurements (CarpetDIEM) I test campaign

Mark C. Anderson ; William J. Doebler ; Kent L. Gee ; Kaylee Nyborg ; Alexandra Loubeau

Check for updates

J. Acoust. Soc. Am. 160, 2119–2130 (2026)
https://doi.org/10.1121/10.0046475

View Online
Export Citation

Articles You May Be Interested In

Investigating sonic booms using impulse metrics
J. Acoust. Soc. Am. (March 2024)

Application of turbulence filters on PCBoom predictions for two NASA flight test campaigns
J. Acoust. Soc. Am. (October 2023)

Atmospheric effects on the propagation of sonic booms utilizing ray tracing methods
J. Acoust. Soc. Am. (March 2024)

14 September 2026 20:23:01

ASA
LEARN MORE
Advance your science and career as a member of the
Acoustical Society of America

ASA
ACOUSTICAL SOCIETY OF AMERICA

JASA ARTICLE

Comparing measured sonic boom turbulence-induced variability with computational models for the Carpet Determination in Entirety Measurements (CarpetDIEM) I test campaign

Mark C. Anderson,[1,a)] William J. Doebler,[2] Kent L. Gee,[1] Kaylee Nyborg,[1] and Alexandra Loubeau[2]
[1]*Department of Physics and Astronomy, Brigham Young University, Provo, Utah 84602, USA*
[2]*Flight Vehicle Acoustics Branch, NASA Langley Research Center, Hampton, Virginia 23681, USA*

ABSTRACT:
When a sonic boom propagates through the atmospheric boundary layer, atmospheric turbulence distorts the waveform, producing stochastic variations over short distances. Accurate prediction of this variability is essential because turbulence affects both waveform characteristics and human-perception metrics used to evaluate supersonic overflights. During NASA's 2019 Carpet Determination in Entirety Measurements I (CarpetDIEM I) flight test campaign, Brigham Young University deployed a 120 m (400 ft) linear array with seven microphones to quantify turbulence-induced variability of sonic boom waveforms, spectra, and metrics. In this study, state-of-the-art models PCBoom and KZKFourier are combined with two weather models, CFSv2 and ERA5, to predict metric variability and compare results with CarpetDIEM I measurements. Depending on the metric and confidence interval considered, prediction success ranges between about 30% and 80%. For the perceived level metric, the prediction successes for the mean and standard deviation were 30%–48% and 52%–65% respectively, depending on the weather model. This compares favorably with the Sonic Booms in Atmospheric Turbulence prediction success results of 45% and 71% for the perceived level mean and standard deviation respectively, using data reported by Stout, Sparrow, and Blanc-Benon [(2021). J. Acoust. Soc. Am. **149**, 3250–3260].
Published 2026. This is a work of the U.S. Government and is not subject to copyright protection in the United States. https://doi.org/10.1121/10.0046475

(Received 26 January 2026; revised 18 August 2026; accepted 19 August 2026; published online 9 September 2026)
[Editor: Con Doolan] Pages: 2119–2130

14 September 2026 20:23:01

I. INTRODUCTION

Turbulence-induced variability has long been known to affect sonic boom signatures (Hilton *et al.*, 1964, 1966; Hubbard *et al.*, 1964). These variations generally include either sharpened or rounded peaks, although a variety of waveform shapes can be measured (Lipkens and Blackstock, 1998; Maglieri and Sothcott, 1990). Because these changes tend to affect the higher frequencies contained within the sonic boom signature, human perception-based metrics can be strongly affected by these variations (Stout, 2018; Bradley *et al.*, 2020; Durrant *et al.*, 2022). As these metrics are anticipated to play a central role in future certification of civil supersonic aircraft (Loubeau *et al.*, 2015; Loubeau and Page, 2018), understanding turbulence effects is critical for determining the variability in final measurements. The purpose of this paper is to provide measured results from a field test campaign and assess the accuracy of state-of-the-art modeling tools in simulating the variability.

Recent NASA supersonic flight test campaigns have either noted or directly studied turbulence-induced variability (Bradley *et al.*, 2020; Durrant *et al.*, 2022; Page *et al.*, 2015; Doebler, 2017). One of these flight tests was the Superboom Caustic Analysis and Measurement Program (SCAMP) (Page *et al.*, 2015). Although measurements of atmospheric turbulence were not the primary goal, Doebler (2017) analyzed turbulence effects using a subset of the SCAMP dataset that had straight, constant Mach number, passes over the 3-km (10 000-ft) linear microphone array. That analysis estimated the number of microphone measurements of a supersonic aircraft flyover required to achieve reasonably converged confidence interval widths for perception metrics. The final recommended number of microphones by Doebler (2017) is between 7 and 10 measurements using the SCAMP array, with microphone spacing of about 38 m (125 ft). Whether a smaller spacing would be acceptable is not answerable using the SCAMP array because there were no closer-spaced microphones.

The most extensive work performed on studying sonic booms in atmospheric turbulence to-date was the Sonic Booms in Atmospheric Turbulence (SonicBAT) campaign, which studied the effects of turbulence in both dry and humid environments along with simultaneous atmospheric turbulence measurements. A primary purpose of the SonicBAT project was to develop and validate modeling tools for statistically describing turbulence effects (Stout, 2018; Bradley

[a)]Email: mark.anderson@byu.net

Published 2026. This is a work of the U.S. Government and is not subject to copyright protection in the United States.

et al., 2020; Stout *et al.*, 2021). The KZKFourier model for propagation through turbulence was developed during SonicBAT and is described in detail by Stout (2018). In short, the KZKFourier model uses random Fourier modes to produce a turbulent atmosphere through which an initial plane wave signature is propagated using a numerical solution to the Khokhlov–Zabolotskaya–Kuznetsov (KZK) equation (Hamilton and Blackstock, 2024). The KZKFourier results were validated for the SonicBAT test campaign (Stout *et al.*, 2021), where it was found that the simulated mean perceived level (PL) (Stevens, 1972; Shepherd and Sullivan, 1991) values were accurately captured 45% of the time to within 95% of the measurement uncertainty and simulated PL standard deviations were accurately captured 71% of the time to the same confidence limit.[1] For both the mean and standard deviations, there was no observed positive or negative bias when comparing simulations to measurements. Although encouraging, the KZKFourier model has not yet been tested on a different dataset, which is an important next step to demonstrating its generality.

Although simulations suggest that turbulence-induced variability will have a smaller impact on shaped booms (Stout and Sparrow, 2018, 2022; Carr *et al.*, 2022), the overall trends between N-waves and shaped booms are similar, and there remain outliers in both cases (Stout, 2018). Thus, it is relevant to study turbulence-induced variability for N-waves because the results inform trends for shaped booms.

The purpose of this paper is to compare measured and modeled turbulence-induced variability using data from a recent supersonic flight test campaign. The modeling is performed using PCBoom (Lonzaga *et al.*, 2025), KZKFourier, and simulated turbulence parameters from two different atmospheric models. PCBoom uses atmospheric raytracing and simulated nonlinear propagation via the Burgers equation to model sonic boom footprints and waveforms. In this paper's applications, it is used to predict a waveform at the top of the atmospheric boundary layer for input into KZKFourier. The atmospheric models used as input into KZKFourier are the Climate Forecast System Version 2 (CFSv2) (Saha *et al.*, 2014) and the European Centre for Medium-Range Weather Forecasts (ECMWF) Reanalysis v5 (ERA5) (Hersbach *et al.*, 2020). The test campaign from which acoustic data are obtained is the Carpet Determination in Entirety Measurements I (CarpetDIEM I) test performed in July–August 2019 (Durrant *et al.*, 2022). Because simultaneous turbulence data were not gathered during CarpetDIEM I, the sonic boom modeling in this paper uses primarily simulated inputs. Two exceptions to this are the use of as-flown trajectories and measured stratified atmosphere data for ray tracing to the top of the atmospheric boundary layer.

This paper proceeds as follows. The CarpetDIEM I measurements are discussed in Sec. II. Section III then includes a discussion of modeled turbulence parameters during CarpetDIEM I with outputs from the two different atmospheric models. In Sec. IV, the subject of placing uncertainty bounds on perception metric standard deviation estimates is discussed. Section V then contains an analysis of the measured metric variability during the CarpetDIEM I test campaign. Last, Sec. VI contains the comparison between measured and modeled metric values before conclusions are presented in Sec. VII.

II. MEASUREMENTS

The NASA CarpetDIEM I test campaign occurred in July–August 2019 (Durrant *et al.*, 2022) with the primary goal of testing logistics for future X-59 flights that will occur in the same desert area near Edwards Air Force Base and NASA Armstrong Flight Research Center (AFRC). Sonic booms were produced by an F/A-18A aircraft flying at about Mach 1.3 at an altitude of about 10.7 km (35 000 ft). Over three flight days, there were 6 flights, resulting in 23 total passes over a ground microphone array.

At one of the ground measurement stations, located undertrack and nearly orthogonal to the anticipated carpet centerline, a linear array of seven microphones was spaced over 120 m (400 ft) to study the effects of atmospheric turbulence on the sonic booms, as shown in Fig. 1 (Durrant *et al.*, 2022; Anderson *et al.*, 2024a). Such a microphone array, deployed with the explicit intention to measure the effects of atmospheric turbulence on sonic boom signatures and metrics, is hereafter referred to in this paper by the term "turbulence array." Because the array size is small compared with the aircraft altitude, it is assumed that atmospheric turbulence effects are the primary contributor to variability across the array and that any off-center flight effects are negligible. In the turbulence array, the shortest spacing was 15 m (50 ft), consistent with the conclusions of Maglieri *et al.* (2014) which, based on the work of Roberts *et al.* (1967), suggested that the measurements must be at least 15 m (50 ft) apart to eliminate correlation between measurements. This is quantified in Fig. 2, which shows the magnitude of the difference in PL between microphone pairs across all booms used in this paper. The individual circles are single microphone pair difference values, and the red line indicates the median value for each distance. Assuming the oscillations at larger distances would smooth out with more data, then by 15 m the median PL difference due to atmospheric turbulence effects appears to be within 1–2 dB of its asymptotic value while the peak differences occur between 30 and 90 m separation. Thus, although using a combination of 15- and 30-m spacings between adjacent microphones in this analysis may slightly underestimate the overall variability, it is not anticipated to be a dramatic underestimate. Because the median difference also appears to approach its asymptotic value, it is concluded that the array is of sufficient length to capture the variability. It is worth noting, however, that the proper spacing for this analysis may not be universal, as Loubeau *et al.* (2021) found that for simulated low booms, 30-m spacing would appear more appropriate. Additionally, because the 15- and 30-m spacings appear to have similar difference distributions in Fig. 2, the different spacings are treated identically in all statistical analyses in this paper. Overall, the determination of

14 September 2026 20:23:01

https://doi.org/10.1121/10.0046475

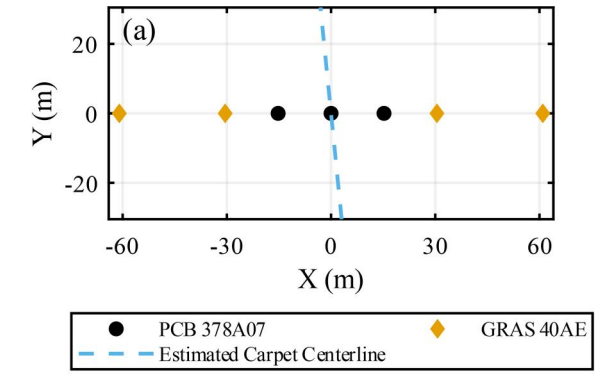




FIG. 1. The microphone array deployed by BYU during the CarpetDIEM test campaign. (a) The microphone locations, indicating the two different microphone types deployed. (b) A photograph of the data acquisition unit and the center microphone.

the appropriate microphone spacing and array dimensions for both N-waves and low booms is an important aspect of ongoing research, where lessons learned from fielding this array are already being applied (Nyborg *et al.*, 2025a, 2025b).

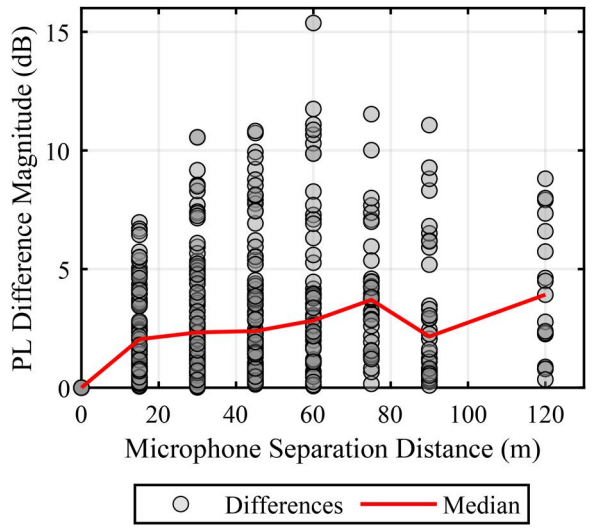


FIG. 2. The magnitude of the difference in PL between microphone pairs at the CarpetDIEM I turbulence array.

Due to hardware constraints, two types of 1/2-inch microphones were used at this location: three PCB 378A07 microphones and four GRAS 40AE microphones. Each microphone was placed inverted over a circular plastic ground plate and shrouded in a domed windscreen (Anderson *et al.*, 2022; James *et al.*, 2020). The GRAS 40AE microphones have a low-frequency cutoff that does not allow accurate representation of the linear ramp portions of the waveform, i.e., between the shocks. This was corrected for in all measurements via digital pole-shift filtering (Rasband *et al.*, 2023; Marston, 2008). Additionally, high-frequency contaminating noise was removed from the metric calculations using the methods in Anderson *et al.* (2024b).

Additionally, owing to the higher sensitivity of the GRAS 40AE microphones, some measurements experienced peak-pressure clipping. These recordings have been omitted from the analyses in this paper. Because the PCB 378A07 channels never clipped, it is assumed that metric statistics are adequately captured. The number of valid recordings for each pass is used to create confidence intervals used throughout this paper. For discussions of how minorly-clipped sonic booms may still be usable for metric calculations, see Gee *et al.* (2024) and Anderson (2026).

Figure 3 shows sonic boom data recorded at each microphone for a single pass. Figure 3(a) shows all seven waveforms. Note that some are more rounded, while others are more spiked. These waveform characteristics have a direct impact on the spectrum, as shown in Fig. 3(b). For example, the waveform measured at 60 m (200 ft) is more rounded and hence has less high-frequency content while the waveforms measured at −15 m (−50 ft) and −60 m (−200 ft) are more spiked and therefore have more high-frequency content. Although the spectra all agree well at frequencies below about 30 Hz, it is the higher frequencies that primarily affect the human-perception metrics, as shown in Fig. 3(c). These curves are the specific loudness spectra used during the calculation of the PL for each boom (Stevens, 1972). Note that the dominant frequencies are now around 50–1000 Hz, which coincides with much of the variability observed in Fig. 3(b). Thus, atmospheric turbulence effects can drive large changes in the sonic boom human-perception metrics, as also observed by Bradley *et al.* (2020), Stout *et al.* (2021), and Carr *et al.* (2022).

III. MODELED TURBULENCE PARAMETERS

Because real-time turbulence measurements were not performed during CarpetDIEM I, the turbulence input parameters for KZKFourier are obtained from two atmospheric models. The first is the CFSv2 (Saha *et al.*, 2014) and the second is the ERA5 (Hersbach *et al.*, 2020). The first model, CFSv2, is an operational forecast product from the National Oceanic and Atmospheric Administration. It ingests observational data within a few hours prior to the forecast time and uses a coupled model for the atmosphere, ocean, land, and sea ice states. The second model, ERA5, is a reanalysis product from ECMWF. A reanalysis utilizes

14 September 2026 20:23:01

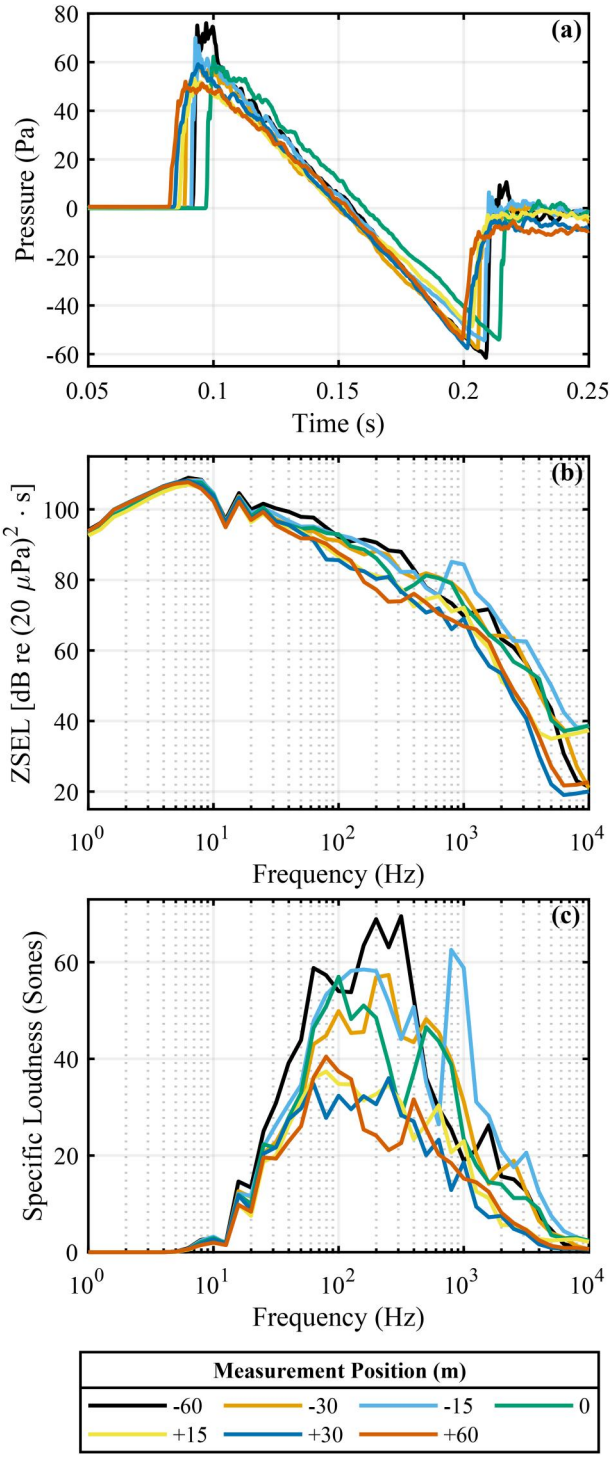


FIG. 3. Sample data from one of the passes over the array (Pass 11). (a) The seven waveforms recorded across the array. (b) The flat-weighted sound exposure level spectrum corresponding to each waveform. (c) The loudness spectrum for each waveform.

both observations and short-term forecasts as input, combining them through a data assimilation process to minimize output uncertainty. Its preliminary data are made available with a 5-day latency, and data are finalized 2–3 months after first appearing. The relaxed time constraint in ERA5 allows for more and better-calibrated observations to be used. Although a full description of these complex models' outputs is beyond the scope of this paper, the turbulence parameters needed for KZKFourier can be selected or derived by the user given a location and time span. Because there is no conclusive answer for whether CFSv2 or ERA5 is better suited for sonic boom modeling (Doebler and Loubeau, 2023; Lympany and Page, 2024), both are used throughout this paper with no attempt to definitively state if one model is preferred. The comparison, however, helps provide a sense of variability due to the choice of weather model.

With inputs from the atmosphere models, KZKFourier uses the turbulence theory of Ostashev and Wilson (Wilson, 2000; Ostashev and Wilson, 2015). This model is a von Kármán spectral model that accounts for shear and buoyancy effects. Among the Ostashev and Wilson turbulence parameters used in KZKFourier, there are two that stand out as being of particular importance (Bradley *et al.*, 2020; Stout *et al.*, 2021). These are the atmospheric boundary layer (ABL) height and the root mean square (RMS) turbulence wind speed, denoted as σ_{vector}. Turbulence is often described as a split between scalar turbulence (temperature fluctuations) and vector turbulence (wind fluctuations), with both being accounted for in KZKFourier. Despite its name, the quantity σ_{vector} is a scalar, and the term "vector" denotes that this quantity is the standard deviation of the vector turbulence magnitude. This quantity is calculated as

$$\sigma_{\text{vector}} = \sqrt{3.0u_*^2 + 0.35w_*^2}, \tag{1}$$

where u_* is the friction velocity and w_* is the mixed-layer velocity scale.[2] (Bradley *et al.*, 2020; Wilson 2000).

The CFSv2 and ERA5 outputs are directly compared over the duration of CarpetDIEM I in Fig. 4. Figure 4(a) shows the estimated ABL height as a function of time. The times of each of the six flights are indicated with the dashed red lines. The CFSv2 output tends to estimate an ABL height that is greater than the ERA5 output. Figure 4(b) shows the same type of comparison for σ_{vector}, where again CFSv2 estimates greater values than ERA5. However, the differences at the σ_{vector} peaks appear more constant than the ABL height differences. It is important to note that, because CFSv2 predicts greater values (and therefore greater overall turbulence), KZKFourier simulations produced using the CFSv2 weather data are expected to have lower average metric values than the ERA5 results because greater turbulence is associated with longer sonic boom rise times and reduced high-frequency levels on average (Lipkens and Blackstock, 1998; Lonzaga, 2023). The greater turbulence values are also expected to affect the metric variability, but definitive statements are hard to make beforehand because the variability is expected to increase and then decrease with propagation distance (Carr *et al.*, 2022).

IV. QUANTIFYING STANDARD DEVIATION UNCERTAINTY

Because sonic boom metric estimates based on a finite number of array measurements are inherently uncertain,

14 September 2026 20:23:01

https://doi.org/10.1121/10.0046475

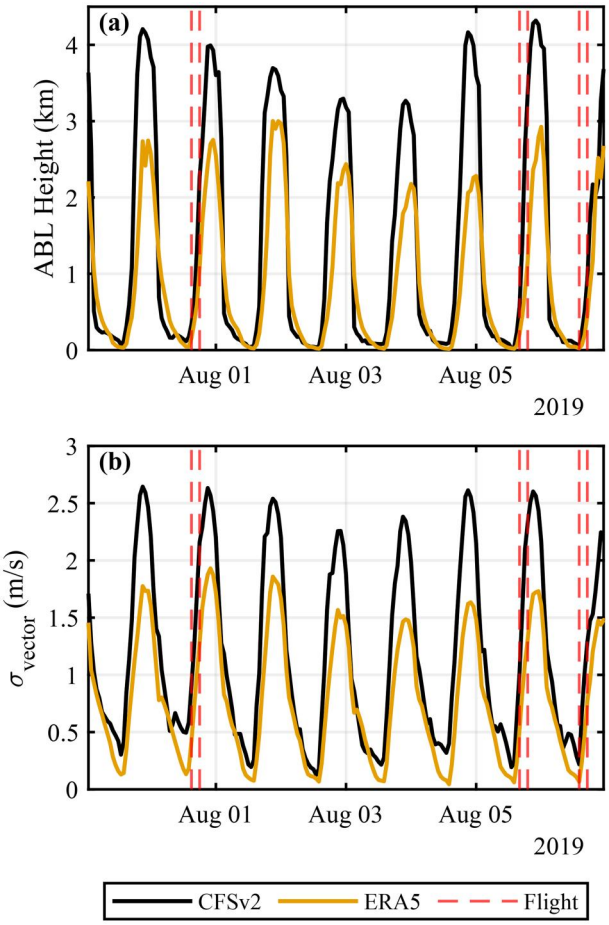


FIG. 4. Comparing the CFSv2 and ERA5 outputs for (a) atmospheric boundary layer height and (b) the standard deviation of the vector turbulence magnitude. Dashed red lines indicate flight times.

confidence intervals should be reported. This was investigated as part of the SonicBAT program (Bradley *et al.*, 2020; Stout *et al.*, 2021), and a brief discussion is given here as well.

In many cases, the variability due to atmospheric turbulence is reported as a standard deviation of measured quantities (Bradley *et al.*, 2020; Carr *et al.*, 2022; Averiyanov *et al.*, 2011; Stout *et al.*, 2021). The confidence bounds on a standard deviation calculated using a finite number of data points can be calculated as (Sheskin, 2000)

$$\sqrt{\frac{(n-1)s^2}{\chi^2_{[1-(\alpha/2)]}}} \leq \sigma \leq \sqrt{\frac{(n-1)s^2}{\chi^2_{(\alpha/2)}}}, \tag{2}$$

where σ is the true standard deviation of the population, s is the sample standard deviation calculated from the data, n is the number of data points, χ^2 represents the chi-square distribution, and α is the confidence ($\alpha = 0.05$ is used to calculate the 95% confidence interval). Note that Eq. (2) assumes an underlying normal distribution and that the values are randomly chosen from that distribution. While Eq. (2) can be used as-is to calculate the confidence bounds on the estimated standard deviation, additional insight into how the uncertainty scales with the number of samples can be gained by normalizing each term by the sample standard deviation,

$$\sqrt{\frac{(n-1)}{\chi^2_{[1-(\alpha/2)]}}} \leq \frac{\sigma}{s} \leq \sqrt{\frac{(n-1)}{\chi^2_{(\alpha/2)}}}. \tag{3}$$

Equation (3) produces normalized multipliers σ/s, which are plotted as a function of the number of measurements in Fig. 5. This figure can be interpreted as follows: given the number of measurements for a supersonic pass across the turbulence array, one can determine the ratio σ/s for the 95% confidence upper and lower bounds. The values are then multiplied by the sample standard deviation to determine the upper and lower 95% confidence bounds on that standard deviation. For example, 10 measurements will have $\sigma/s = [0.688, 1.83]$, and if the sample standard deviation of those 10 measurements is 2.00, then the 95% confidence interval for $\sigma = [1.38, 3.65]$. Note that the upper and lower bounds are not distributed symmetrically about the sample standard deviation. Again, this methodology in Eq. (3) relies on statistically random measurements, which is an assumption that may be violated if the microphones are physically spaced too close to each other. Interpretation of data from Roberts *et al.* (1967) by Maglieri *et al.* (2014) indicates that 15 m (50 ft) spacing, the minimum microphone spacing at CarpetDIEM I, is adequate to ensure that recordings are statistically random.

The standard deviation confidence intervals defined in Eq. (2) rely only on the number of samples and the sample standard deviation. This enables confidence intervals to be placed retroactively on historical standard-deviation estimates, such as those from SonicBAT. Bradley *et al.* (2020) report the standard deviations of PL, Indoor Sonic Boom Annoyance Predictor (ISBAP), and peak overpressure (P_{max}) as functions of RMS wind turbulence (σ_{vector}) and the propagation distance through turbulence. Although σ/s values were calculated and used in the SonicBAT analysis (though not referred to as σ/s), it is useful to see these error

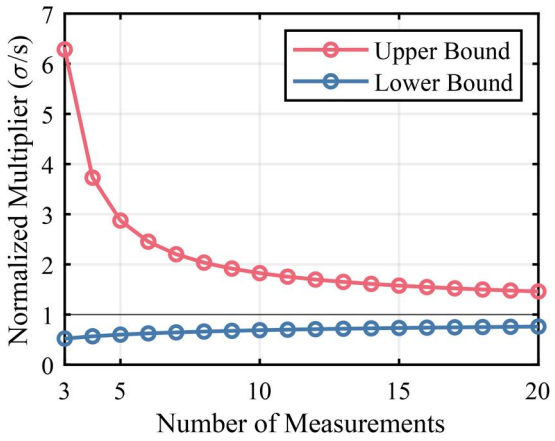


FIG. 5. The normalized multipliers for the 95% confidence bounds on the standard deviation of a dataset with finite data points. These values are multiplied by the sample standard deviation to determine the extent of the 95% confidence bounds.

14 September 2026 20:23:01

bars graphically to better visualize the large uncertainties, even with 16 channels. These results, along with their associated predictions produced during SonicBAT, are reproduced in Fig. 6.

The retroactive error bars in Fig. 6 represent the uncertainty inherent in using a finite number of measurements to estimate the standard deviation. Including these uncertainty bounds is an important element of ensuring that the data are communicated accurately and that comparisons to other sources, like simulations or potentially other measurements, are made more fairly. This was accomplished during SonicBAT and will also be shown below for CarpetDIEM I. Note that the measurement uncertainty presented here does not account for other sources of uncertainty, such as microphone calibration, ambient environmental conditions, background noise, windscreen insertion loss, and data acquisition system settings (Klos, 2025).

Note what appears to be a minor error in the confidence interval calculation for the mean in SonicBAT analyses. Bradley *et al*. (2020) and Stout *et al*. (2021) report using the expression $\pm 2.13\,\sigma/\sqrt{15}$ to calculate the 95% confidence interval for the mean. According to Johnson and Wichern (2007), which is the same edition of the book cited in the SonicBAT works, the denominator should be the square root of the number of observations $(\sqrt{16})$. After making this adjustment, this equation produces identical results to the output of the MATLAB *ttest* function used throughout this paper (MATLAB, version R2023b, The MathWorks Inc., Natick, MA). Whether the SonicBAT analyses were intentionally conservative is never stated; although if it was intentionally conservative, then the numerator would also need to be adjusted accordingly to represent a reduced number of samples.

V. CARPETDIEM I METRIC VARIABILITY

Turbulence-induced variability has a strong impact on human-perception metric values (Bradley *et al*., 2020; Stout, 2018; Doebler, 2017; Durrant *et al*., 2022). The variability observed on a per-boom basis during CarpetDIEM I at the turbulence array is shown in Table I. The estimated RMS wind turbulence (σ_{vector}) and propagation distance through

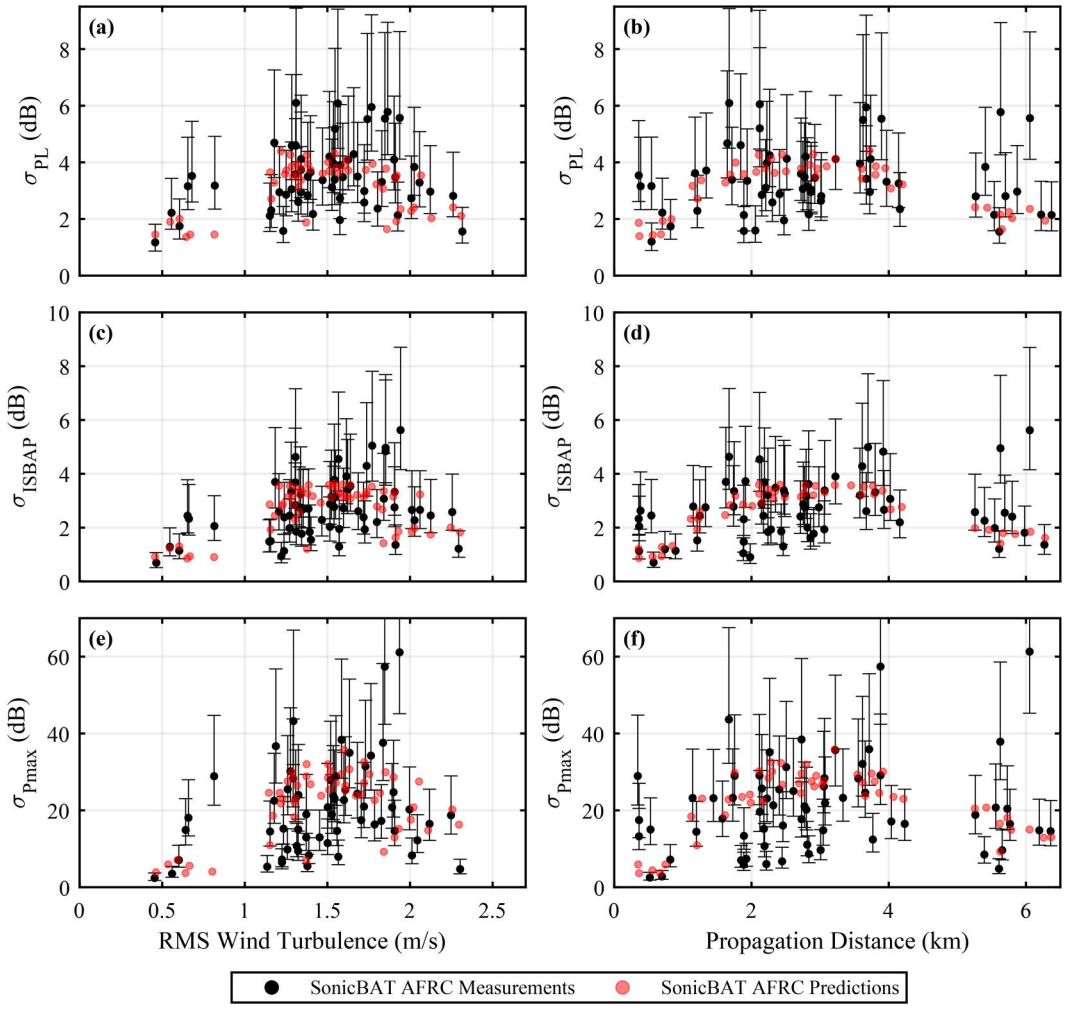


FIG. 6. Retroactive SonicBAT finite-measurement error bars, using data measured at NASA's AFRC. The PL standard deviation is shown as a function of (a) RMS wind turbulence and (b) propagation distance through the ABL. The measurements are compared against predictions made for the SonicBAT conditions. (c), (d) The same results for the ISBAP metric. (e), (f) The same results for the peak overpressure.

14 September 2026 20:23:01

https://doi.org/10.1121/10.0046475

TABLE I. Predicted weather parameters and measurement results from the seven-microphone linear turbulence array deployed during CarpetDIEM I. All confidence bounds are 95%.

Pass	RMS wind turbulence, σ_{vector} (m/s)		Propagation distance (m)		Ray elevation angle (°)		Mics used	Mean PL (dB)	Mean ISBAP (dB)	Mean Pmax (psf)	σ/s	s_{PL} (dB)	s_{ISBAP} (dB)	s_{Pmax} (psf)
	CFSv2	ERA5	CFSv2	ERA5	CFSv2	ERA5								
1	0.99	0.49	800	405	29.7	29.5	7	104.7 ± 1.2	112.0 ± 0.7	1.91 ± 0.16	[0.644, 2.202]	1.3	0.7	0.17
2	1.03	0.53	848	446	30.1	29.9	6	104.4 ± 4.0	111.6 ± 2.4	1.73 ± 0.45	[0.624, 2.453]	3.8	2.3	0.43
3	1.07	0.57	918	500	29.9	29.7	6	102.7 ± 4.3	110.0 ± 3.1	1.64 ± 0.20	[0.624, 2.453]	4.1	2.9	0.19
4	1.11	0.61	1014	568	29.0	28.8	7	99.7 ± 3.3	107.6 ± 1.7	1.31 ± 0.04	[0.644, 2.202]	3.5	1.8	0.05
5	2.20	1.35	4744	2419	30.2	30.1	7	102.9 ± 1.0	110.6 ± 0.7	1.78 ± 0.12	[0.644, 2.202]	1.1	0.8	0.13
6	2.21	1.39	4859	2589	30.2	30.1	7	100.9 ± 1.6	108.5 ± 0.8	1.49 ± 0.15	[0.644, 2.202]	1.7	0.8	0.16
7	2.23	1.44	4773	2655	31.5	31.4	6	104.7 ± 4.3	112.2 ± 3.0	2.06 ± 0.43	[0.624, 2.453]	4.1	2.9	0.41
8	2.24	1.47	4985	2863	30.6	30.4	5	105.5 ± 5.2	113.1 ± 3.7	2.35 ± 0.72	[0.599, 2.874]	4.2	3.0	0.58
9	1.25	0.67	1784	620	29.0	29.8	5	103.3 ± 1.9	110.3 ± 1.7	1.58 ± 0.24	[0.599, 2.874]	1.6	1.4	0.19
10	1.32	0.71	1992	672	29.4	30.2	5	107.3 ± 1.6	113.9 ± 0.8	2.07 ± 0.13	[0.599, 2.874]	1.3	0.6	0.10
11	1.38	0.75	2196	723	29.8	30.6	7	99.2 ± 3.4	107.2 ± 2.4	1.28 ± 0.17	[0.644, 2.202]	3.7	2.6	0.18
12	1.45	0.78	2504	845	28.6	27.9	7	104.5 ± 3.4	111.6 ± 2.1	1.73 ± 0.16	[0.644, 2.202]	3.7	2.3	0.17
13	2.39	1.38	7777	2924	27.2	27.3	5	103.9 ± 5.6	112.9 ± 4.9	2.71 ± 1.00	[0.599, 2.874]	4.5	4.0	0.81
14	2.41	1.41	7684	2994	28.3	28.3	7	101.7 ± 3.3	109.4 ± 2.8	1.75 ± 0.29	[0.644, 2.202]	3.6	3.0	0.31
15	2.43	1.44	8057	3253	27.5	27.5	5	107.6 ± 7.2	114.7 ± 5.1	2.37 ± 0.82	[0.599, 2.874]	5.8	4.1	0.66
16	2.45	1.47	7444	3139	30.6	30.3	3	113.1 ± 7.9	120.1 ± 4.6	4.33 ± 0.89	[0.521, 6.285]	3.2	1.9	0.36
17	0.32	0.10	185	71	26.5	26.5	7	103.9 ± 0.8	112.1 ± 0.5	1.97 ± 0.09	[0.644, 2.202]	0.8	0.5	0.09
18	0.39	0.13	239	80	27.5	27.5	5	108.2 ± 2.1	115.2 ± 1.3	2.16 ± 0.30	[0.599, 2.874]	1.7	1.1	0.24
19	0.46	0.15	311	94	27.1	27.1	4	113.0 ± 5.0	118.7 ± 3.6	2.92 ± 1.10	[0.567, 3.729]	3.1	2.2	0.69
20	1.37	0.84	2670	1315	26.9	26.6	7	91.8 ± 1.5	102.3 ± 1.1	1.13 ± 0.06	[0.644, 2.202]	1.6	1.1	0.07
21	1.39	0.86	2582	1258	30.5	30.2	7	103.2 ± 2.6	110.5 ± 1.6	1.54 ± 0.14	[0.644, 2.202]	2.8	1.7	0.15
22	1.41	0.88	2837	1366	30.1	29.7	7	98.2 ± 1.2	106.9 ± 1.0	1.45 ± 0.08	[0.644, 2.202]	1.3	1.1	0.08
23	1.43	0.89	3060	1475	29.6	29.3	7	99.8 ± 1.7	108.8 ± 1.1	1.79 ± 0.20	[0.644, 2.202]	1.9	1.1	0.22

turbulence (accounting for ray elevation angle) are shown using both the CFSv2 and ERA5 results. The ABL turbulence properties are assumed to be uniform, so the single σ_{vector} value is representative of the full ABL. The propagation distance through turbulence is estimated following the method of Stout (2018, their Fig. 3-1), using the ray elevation angle and ABL height to compute the straight-line distance between the PCBoom-modeled position of the ray at the top of the ABL and its ground intersection. The stratified atmospheric data used in PCBoom were measured by a weather balloon radiosonde (Vaisala, 2017). Additionally, the number of valid microphone recordings used for each measurement is included. The means for PL (dB), ISBAP (dB), and P_{max} (psf) are shown along with their associated 95% confidence intervals, calculated using the MATLAB *ttest* function. The standard deviations for these three metrics are also shown, along with their σ/s intervals, which are identical across all the metrics because the intervals only depend on the sample size and the desired confidence limits.

VI. COMPARISON WITH MODELED RESULTS

To best ascertain whether the modeling tools accurately capture the variability observed in the CarpetDIEM I measurements, simulations were performed according to the flow chart shown in Fig. 7, using a combination of the Enhanced Burgers module of PCBoom 7.4 (Lonzaga *et al.*, 2025) and KZKFourier. As-flown aircraft trajectories coupled with near-field computational fluid dynamics simulations (similar to Loubeau and Doebler, 2019) and stratified atmospheric data from weather balloon radiosonde measurements were input into PCBoom to predict the sonic boom

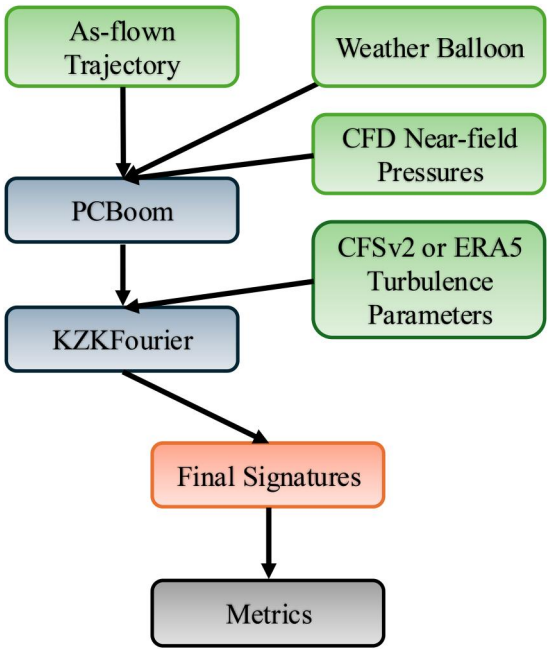


FIG. 7. Schematic showing the process by which the final modeled metrics were produced.

14 September 2026 20:23:01

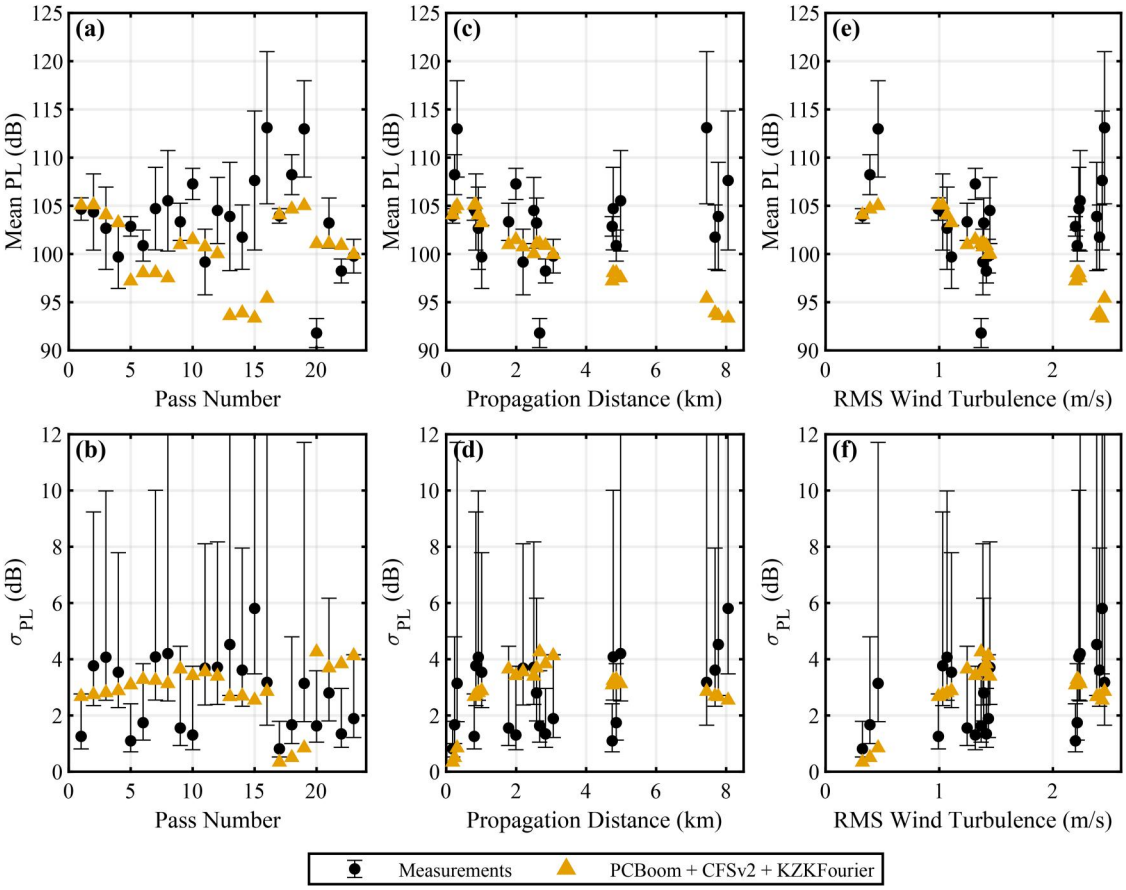


FIG. 8. Comparison between the CarpetDIEM I measurements and PCBoom+CFSv2+KZKFourier predictions as functions of pass number, propagation distance through turbulence, and RMS wind turbulence. The mean PL [(a), (c), (e)] and the standard deviation [(b), (d), (f)] are directly compared, including vertical error bars on the measurements that arise from the finite number of measurements [Eq. (2)].

waveform and entry angle when the boom entered the atmospheric boundary layer. This waveform was then used as an input for KZKFourier (with either CFSv2 or ERA5 modeled turbulence parameters), which was used in its two-dimensional mode to produce distorted waveforms every 0.5 m along a 500-m span. Although KZKFourier can be run in a three-dimensional mode (Stout and Sparrow, 2019), these simulations were performed in two dimensions to reduce the prohibitively high computational expense of running the simulations in three dimensions (Stout, 2018). Using KZKFourier with either CFSv2 or ERA5 modeled turbulence parameters, 20 turbulence realizations were produced, resulting in 20 simulations over 500 m for each pass with each weather model. The metrics for each of the 20 simulations were concatenated as though they were from a single run with a larger span when calculating statistics.

Results using both the PCBoom+CFSv2+KZKFourier and PCBoom+ERA5+KZKFourier combined models are compared directly against measurements in Figs. 8 and 9, respectively. In Figs. 8(a) and 9(a), the mean PL values for each boom measured across the seven-microphone array are compared against the simulations and in Figs. 8(b) and 9(b), the standard deviations are likewise compared. Figures 8 and 9 also show the measured and modeled statistics as functions of the propagation distance through turbulence [Figs. 8(c), 8(d), 9(c), and 9(d)] and the RMS wind turbulence [Figs. 8(e), 8(f), 9(e), and 9(f)], which is identical to σ_{vector}. The differences in propagation distance through atmospheric turbulence are caused by the different ABL height estimates between the CFSv2 and ERA5 models (see Fig. 4). CFSv2 overall suggests greater values of turbulence, which results in greater ABL heights and greater RMS wind turbulence. To maintain visual consistency, the axes between corresponding subplots in Figs. 8 and 9 are kept consistent between the two figures.

It is expected that increased turbulence should cause a decrease in the mean PL (Lonzaga, 2023). This is observed for the simulations in Figs. 8(c), 8(e), 9(c), and 9(e)]. However, the measurements do not show this same trend so clearly. There is a potential explanation for this discrepancy. While each simulation has thousands of data points for averaging, the measurements are simply unable to reach the same reduction in random statistical noise. According to Eq. (3), even if 100 microphones were used, $\sigma/s = [0.878, 1.16]$, indicating that any array of practical size will have a non-negligible amount of uncertainty in assessing the variability. Despite the large uncertainties in the measured values, the simulated values do not always fall within the measurement uncertainty, as is the case for the modeled mean PL results at greater propagation distances and RMS wind turbulence values. This is especially

14 September 2026 20:23:01

https://doi.org/10.1121/10.0046475

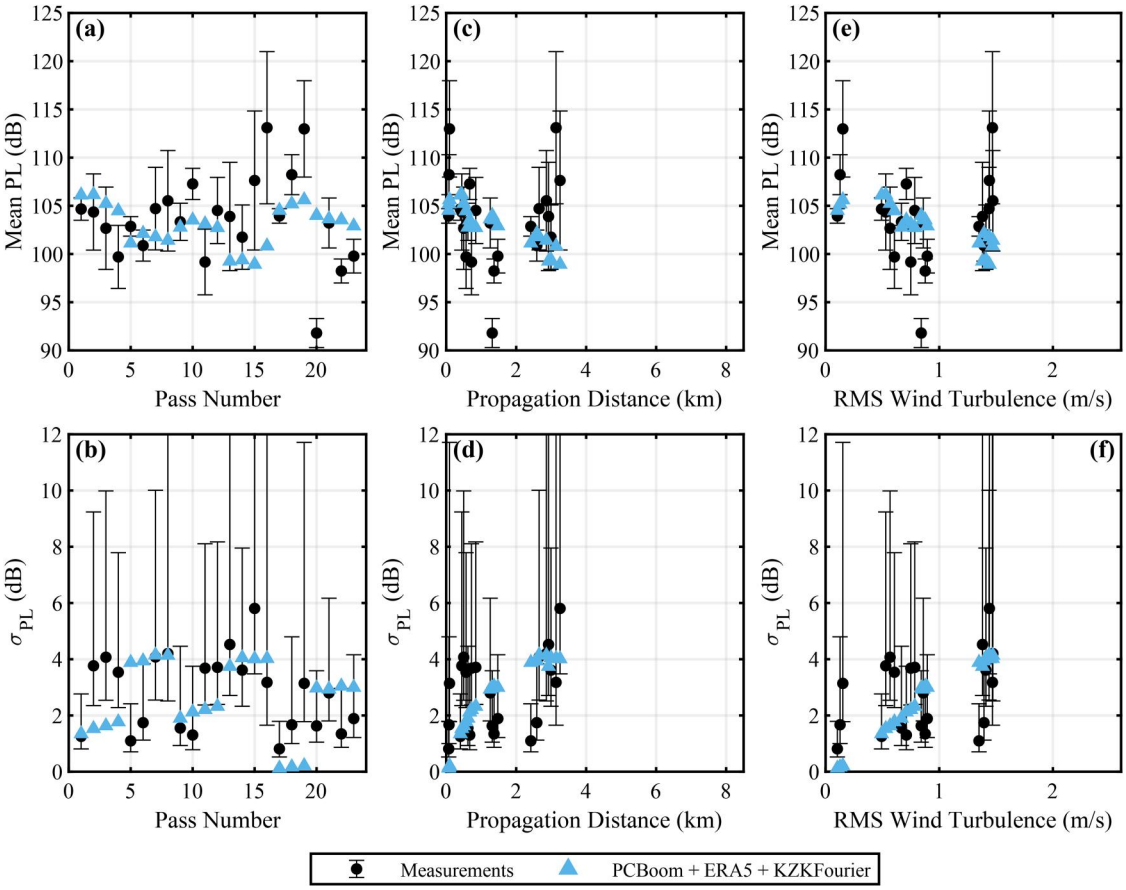


FIG. 9. Comparison between the CarpetDIEM I measurements and PCBoom+ERA5+KZKFourier predictions as functions of pass number, propagation distance through turbulence, and RMS wind turbulence. The mean PL [(a), (c), (e)] and the standard deviation [(b), (d), (f)] are directly compared, including vertical error bars on the measurements that arise from the finite number of measurements [Eq. (2)].

pronounced for the PCBoom+CFSv2+KZKFourier results in Figs. 8(c) and 8(e) but is also observed in the PCBoom+ERA5+KZKFourier results in the corresponding subplots. This difference between the results using the two weather models is likely due to the fact that CFSv2 output greater turbulence levels and thus a more pronounced decrease in the mean PL is expected.

While the expected decrease in mean PL with increased turbulence is not clearly observed in these results, it was observed during SonicBAT for the dataset collected at AFRC (Bradley *et al.*, 2020). It is possible that the trend was more clearly observable for SonicBAT because of the increased number of passes (60) compared to the 23 passes during CarpetDIEM I. It is also worth highlighting that the SonicBAT results at Kennedy Space Center (48 passes) did not produce a clear trend in mean PL with increased turbulence.[3]

It has also been seen in previous simulation work that the PL standard deviation is expected to increase up to a certain propagation distance and then decrease with further propagation (Carr *et al.*, 2022; Bradley *et al.*, 2020, Fig. 6 herein). This is observed in the simulated results using the PCBoom+CFSv2+KZKFourier model in Figs. 8(d) and 8(f). Meanwhile, likely because the ERA5 model predicts a lower ABL height (and corresponding propagation distance through turbulence) along with smaller RMS wind turbulence, the downward portion of the standard deviation trend is not reached in Figs. 9(d) and 9(f). Although the full trend is not observed, the standard deviation appears to reach near its maximum value with propagation distance in Fig. 9(d). As was the case for the mean PL, these trends are not readily observed in the measurements. Indeed, as the estimated propagation distance and RMS wind turbulence values go to zero, the measurements do not have a definitive trend toward zero standard deviation. The reasons for this are unclear.

The mean and standard deviation prediction successes are shown in Fig. 10 for all six metrics given by Loubeau and Page (2018). Metric prediction success is defined as the simulation falling within the 95% confidence intervals for the measurement (i.e., the black bars in Figs. 8 and 9, but calculated individually for each metric). Across metrics, the simulations accurately predict the mean measured value in about 30%–50% of the cases. The standard deviation results are somewhat better at about 30%–80% success, but neither the means nor standard deviations are simulated consistently with great accuracy. Thus, even with large uncertainties, the models used in this paper struggle to accurately predict the measured variability. For comparison, it can be derived from Stout *et al.* (2021, their Figs. 7 and 8) for the SonicBAT study that the prediction

14 September 2026 20:23:01

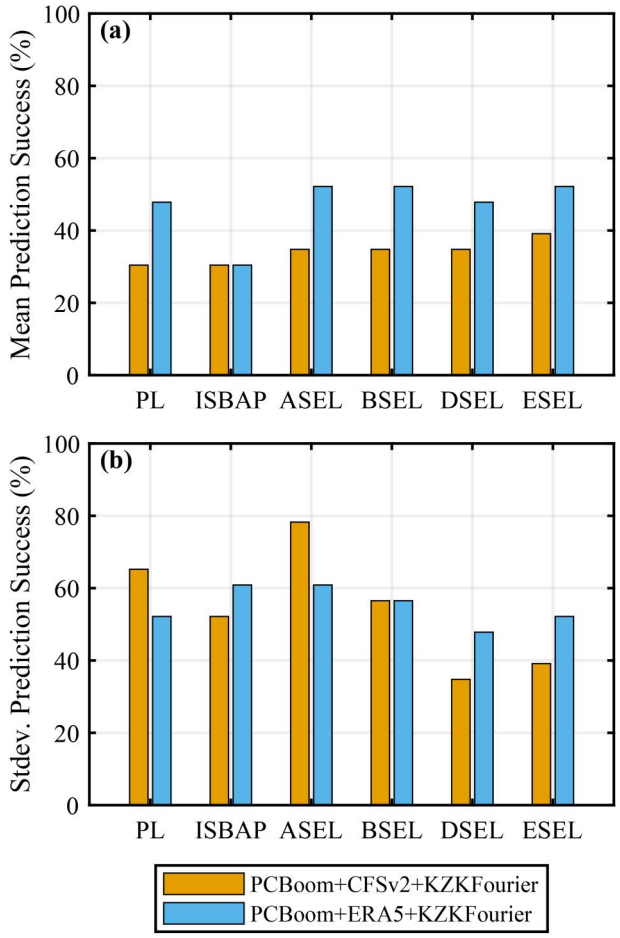


FIG. 10. The prediction success of the PCBoom+CFSv2+KZKFourier and PCBoom+ERA5+KZKFourier simulations, compared to measurements for the (a) mean and (b) standard deviation of each metric. Success is defined by the prediction falling within the 95% confidence region for the measurements estimated using Eq. (2).

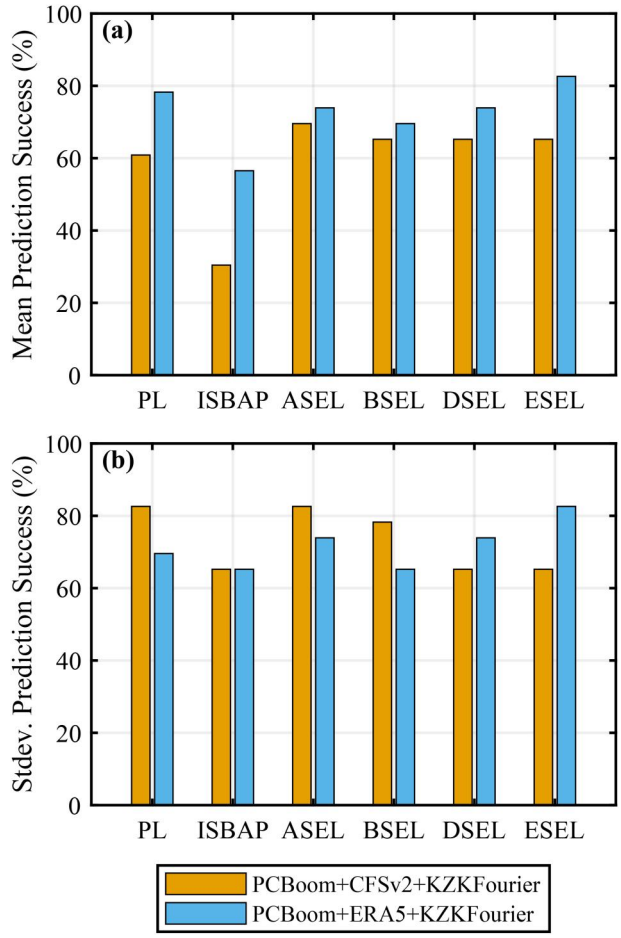


FIG. 11. The prediction success of the PCBoom+KZKFourier+CFSv2 and PCBoom+KZKFourier+ERA5 simulations, compared to measurements for the (a) mean and (b) standard deviation of each metric. Success is defined by the prediction falling within the 99% confidence region for the measurements estimated using Eq. (2).

success for the mean PL was 45% and the PL standard deviation was 71%. It is not clear whether increasing the number of measurements would improve or reduce the prediction success because, while increasing the number of data points does improve the statistical estimates, it also reduces the size of the error bars, potentially making it more difficult for the simulated value to fall within the measurement uncertainty.

If instead, the 99% confidence intervals are used for the measurements, the results are as shown in Fig. 11. The mean values are better simulated when using the ERA5 data, with a mean around 60%–80%, compared to the 30%–80% success rate when using the CFSv2 data.[4] However, the relative success is metric-dependent for the standard deviation, with both models producing results that average around 60%–80%. It is noted, however, that the greater success rate when using the measured 99% confidence intervals is a direct result of the confidence intervals being wider. Further research needs to determine a suitable confidence threshold for mean and standard deviation metric values across sonic boom array measurements. Such a suitable threshold will need to balance accuracy in the sonic boom predictions with uncertainty in the atmospheric measurements.

VII. CONCLUSION

Measurements from a seven-microphone linear array deployed during the NASA CarpetDIEM I sonic boom test campaign have been shown and compared against modeled results. These models included PCBoom (using as-flown trajectory data and measured weather balloon data) for signature evolution and propagation until the booms reach the atmospheric boundary layer. KZKFourier was then used to simulate propagation through the atmospheric boundary layer, with turbulence parameters output by CFSv2 and ERA5.

A method for calculating error bars to be placed on metric standard deviations is proposed and recommended for future use when plotting data. This method relies only on the number of microphones and assumes that they are spaced sufficiently far apart so that the turbulence effects are random. For historical measurement arrays that meet this randomness criterion, retroactive error bars can be placed on the standard deviation estimates.

When comparing the measured CarpetDIEM I results and the modeled results, the prediction accuracy falls within

14 September 2026 20:23:01

about 30%–80%, varying across metric type. These results can be compared directly against SonicBAT results as reported by Stout *et al.* (2021). They had a prediction accuracy of 45% for the mean PL, while in this paper a value of 30%–48% was found, depending on the weather model. Stout *et al.* (2021) also had a prediction accuracy of 71% for the PL standard deviation while a value of 52%–65% was found in this paper. While the overall success rates are therefore similar between CarpetDIEM I and SonicBAT, these percentages are still not as high as could be hoped for. At present, it is not yet known which of the tools or inputs (PCBoom, KZKFourier, or CFSv2/ERA5) needs the most immediate attention to improve modeling accuracy.

The topic of atmospheric turbulence effects on sonic booms will become increasingly important as measurements are made of low-boom aircraft and decisions will need to be made about how to distribute microphones across the measurement domain. It is recommended to obtain simultaneous turbulence and other meteorological measurements during the flights along with accurate near-field pressure data around the aircraft, as those could improve the prediction accuracy. It is also recommended to compare final modeled sonic boom results using both measured and simulated turbulence quantities to determine the degree to which simulated turbulence quantities can be trusted for the many future sonic boom flight campaigns that will occur.

ACKNOWLEDGMENTS

This work was supported by NASA Langley Research Center through National Institute of Aerospace and Analytical Mechanics Associates. Substantial portions of this paper are reproduced from the Ph.D. dissertation of M. C. A. (Anderson, 2026). We thank all those at the NASA Langley Research Center and Brigham Young University who provided feedback on the manuscript; and two anonymous reviewers for their prompt and thorough feedback on this manuscript, which led to many meaningful changes to the text and figures and contributed to the clarity and scientific value of the manuscript. NAVAIR Public Release 2026-0064 Distribution Statement A — Approved for public release; distribution is unlimited.

AUTHOR DECLARATIONS

Conflict of Interest

The authors have no conflicts of interest to disclose.

DATA AVAILABILITY

The data that support the findings of this study are available on request from the corresponding author. The data are not publicly available due to security restrictions.

[1]Those percentages are not directly reported by Stout *et al.* (2021) but can be derived from their Figs. 7 and 8.

[2]The mixed-layer velocity scale is not natively output from the weather models, but it can be derived using other native outputs (sensible heat flux, ABL height, surface pressure, and surface temperature).

[3]Stout *et al.* (2021) state that absorption complications caused by clouds were a possible issue with the Kennedy Space Center analysis.

[4]Among these results, the mean ISBAP using CFSv2 weather data is the only metric that fails to capture more simulation points within the larger 99% confidence intervals.

Anderson, M. C. (**2026**). "Sonic booms from rockets: Measurements and modeling," Ph.D. dissertation, Brigham Young University, Provo, UT.

Anderson, M. C., Gee, K. L., Durrant, J. T., Loubeau, A., Doebler, W. J., and Klos, J. (**2024a**). "Recommendations for sonic boom community noise testing measurement and analysis," Proc. Mtgs. Acoust. **50**, 040008.

Anderson, M. C., Gee, K. L., Durrant, J. T., Loubeau, A., Doebler, W. J., and Klos, J. (**2024b**). "Reducing contaminating noise effects when calculating low-boom loudness levels," J. Acoust. Soc. Am. **155**, 3889–3899.

Anderson, M. C., Gee, K. L., Novakovich, D. J., Mathews, L. T., and Jones, Z. T. (**2022**). "Comparing two weather-robust microphone configurations for outdoor measurements," Proc. Mtgs. Acoust. **42**, 040005.

Averiyanov, M., Ollivier, S., Khokhlova, V., and Blanc-Benon, P. (**2011**). "Random focusing of nonlinear acoustic N-waves in fully developed turbulence: Laboratory scale experiment," J. Acoust. Soc. Am. **130**(6), 3595–3607.

Bradley, K. A., Hobbs, C. M., Wilmer, C. B., Sparrow, V. W., Stout, T. A., Morgenstern, J. M., Underwood, K. H., Maglieri, D. J., Cowart, R. A., Collmar, M. T., Shen, H., and Blanc-Benon, P. (**2020**). "Sonic Booms in Atmospheric Turbulence (SonicBAT): The influence of turbulence on shaped sonic booms," Report No. NASA/CR-2020-220509.

Carr, A. N., Lonzaga, J. B., and Miller, S. A. E. (**2022**). "Numerical prediction of loudness metrics for N-waves and shaped sonic booms in kinematic turbulence," J. Acoust. Soc. Am. **151**, 3580–3593.

Doebler, W. J. (**2017**). "The minimum number of ground measurements required for narrow sonic boom metric 90% confidence intervals," M.S. thesis, The Pennsylvania State University, University Park, PA.

Doebler, W., and Loubeau, A. (**2023**). "A procedure for obtaining forecast turbulence parameters in the atmospheric boundary layer for acoustic propagation," J. Acoust. Soc. Am. **154**, A147. [Abstract only. Slides available from NASA Technical Reports Server Document ID 20230017081. https://ntrs.nasa.gov/citations/20230017081].

Durrant, J. T., Gee, K. L., Anderson, M. C., Mathews, L. T., Rasband, R. D., and Novakovich, D. J. (**2022**). "An overview of Brigham Young University's participation in NASA's CarpetDIEM campaign," Proc. Mtgs. Acoust. **43**, 045002.

Gee, K. L., Anderson, M. C., Durrant, J. T., Blaine, J. D., Nyborg, K., and Sorrell, A. K. (**2024**). "Sonic boom analyses in support of improved X-59 community noise testing," Report No. NASA/CR-20240008985.

Hamilton, M. F., and Blackstock, D. T. (**2024**). *Nonlinear Acoustics* (Springer, New York).

Hersbach, H., Bell, B., Berrisford, P., Hirahara, S., Horányi, A., Muñoz-Sabater, J., Nicolas, J., Peubey, C., Radu, R., Schepers, D., Simmons, A., Soci, C., Abdalla, S., Abellan, X., Balsamo, G., Bechtold, P., Biavati, G., Bidlot, J., Bonavita, M., De Chiara, G., Dahlgren, P., Dee, D., Diamantakis, M., Dragani, R., Flemming, J., Forbes, R., Fuentes, M., Geer, A., Haimberger, L., Healy, S., Hogan, R. J., Hólm, E., Janisková, M., Keeley, S., Laloyaux, P., Lopez, P., Lupu, C., Radnoti, G., de Rosnay, P., Rozum, I., Vamborg, F., Villaume, S., and Thépaut, J.-N. (**2020**). "The ERA5 global reanalysis," Q J. R Meteorol. Soc. **146**(730), 1999–2049.

Hilton, D. A., Huckel, V., and Maglieri, D. J. (**1966**). "Sonic-boom measurements during bomber training operations in the Chicago area," Report No. NASA-TN-D-3655, NASA Langley Research Center.

Hilton, D. A., Huckel, V., Steiner, R., and Maglieri, D. J. (**1964**). "Sonic-boom exposures during FAA community-response studies over a 6-month period in the Oklahoma City area," Report No. NASA-TN-D-2539, NASA Langley Research Center.

Hubbard, H. H., Maglieri, D. J., Huckel, V., and Hilton, D. A. (**1964**). "Ground measurements of sonic-boom pressures for the altitude range of 10 000 to 75 000 feet," Report No. NASA-TN-D-2539, NASA Langley Research Center.

James, M., Salton, A., Calton, M., Downing, M., Gee, K. L., and McInerny, S. A. (**2020**). "Commercial space operations noise and sonic boom measurements," Contractor's Final Report No. ACRP Project 02-81. https://www.trb.org/ACRP/Blurbs/180769.aspx (Last viewed April 9, 2025).

14 September 2026 20:23:01

Johnson, R. A., and Wichern, D. W. (**2007**). *Applied Multivariate Statistical Analysis*, 6th ed. (Pearson Prentice Hall, Upper Saddle River, NJ).
Klos, J. (**2025**). "Uncertainty quantification for empirical X-59 sonic boom loudness levels," Report No. NASA/TM-20250000107.
Lipkens, B., and Blackstock, D. T. (**1998**). "Model experiment to study sonic boom propagation through turbulence: I. General results," J. Acoust. Soc. Am. **104**, 1301–1309.
Lonzaga, J. B., Page, J. A., Downs, R. S., Son, S. R., Ahearn, M. J., Loubeau, A., and Doebler, W. J. (**2025**). "PCBoom 7 technical reference," 2nd ed., Report No. NASA TM-20250003228.
Lonzaga, J. B. (**2023**). "Multiple scattering theory for modeling sonic booms in atmospheric turbulence," J. Acoust. Soc. Am. **154**, 3078–3088.
Loubeau, A., and Doebler, W. J. (**2019**). "Comparison of sonic boom noise metrics from predictions and measurements under low atmospheric turbulence conditions," J. Acoust. Soc. Am. **145**, 1899. [Abstract only. Slides available from NASA Technical Reports Server Document ID 20200005310. https://ntrs.nasa.gov/citations/20200005310].
Loubeau, A., Doebler, W. J., Wilson, S. R., Ballard, K., Coen, P. G., Naka, Y., Sparrow, V. W., Kapcsos, J., Page, J. A., Downs, R. S., Lemaire, S., and Liu, S. R. (**2021**). "Developing certification procedures for quiet supersonic aircraft using shaped sonic boom predictions through atmospheric turbulence," J. Acoust. Soc. Am. **149**, A102. [Abstract only. Slides available from NASA Technical Reports Server Document ID 20210015147. https://ntrs.nasa.gov/citations/20210015147].
Loubeau, A., Naka, Y., Cook, B. G., Sparrow, V. W., and Morgenstern, J. M. (**2015**). "A new evaluation of noise metrics for sonic booms using existing data," AIP Conf. Proc. **1685**, 090015.
Loubeau, A., and Page, J. (**2018**). "Human perception of sonic boom from supersonic aircraft," Acoust. Today **14**(3), 23–30.
Lympany, S. V., and Page, J. A. (**2024**). "The influence of atmospheric variability on predicted sonic boom metrics," J. Acoust. Soc. Am. **155**, A256. [Abstract only. Slides available from NASA Technical Reports Server Document ID 0240005397. https://ntrs.nasa.gov/citations/20240005397].
Maglieri, D. J., Bobbitt, P. J., Plotkin, K. J., Shepherd, K. P., Coen, P. G., and Richwine, D. M. (**2014**). "Sonic boom: Six decades of research," Report No. NASA-SP-2014-622.
Maglieri, D. J., and Sothcott, V. E. (**1990**). "Summary of sonic boom rise times observed during FAA community response studies over a 6-month period in the Oklahoma City area," Report No. NASA-CR-4277.
Marston, T. M. (**2008**). "Diffraction correction and low-frequency response extension for condenser microphones," M.S. thesis, The Pennsylvania State University, University Park, PA.
Nyborg, K., Gee, K. L., and Loubeau, A. (**2025a**). "Variation in sonic boom metrics due to atmospheric turbulence during CarpetDIEM III," in *AIAA AVIATION Forum and ASCEND*.
Nyborg, K., Wettstein, I. D., Gee, K. L., and Loubeau, A. (**2025b**). "Metric variability in a fine-resolution microphone array at NASA Quest Mission Phase 2 Dry Run," J. Acoust. Soc. Am. **158**, A119.
Ostashev, V. E., and Wilson, D. K. (**2015**). *Acoustics in Moving Inhomogeneous Media* (CRC, Boca Raton, FL), pp. 193–205.
Page, J., Plotkin, K. J., Hobbs, C., Sparrow, V., Salamone, J., Cowart, R., Salamone, J., Elmer, K., Welge, H. R., Ladd, J., Maglieri, D., and Piacsek, A. (**2015**). "Superboom Caustic Analysis and Measurement Program (SCAMP) Final Report," Report No. NASA/CR-2015-218871.
Rasband, R. D., Gee, K. L., Gabrielson, T. B., and Loubeau, A. (**2023**). "Improving low-frequency response of sonic boom measurements through digital filtering," JASA Express Lett. **3**(1), 014802.
Roberts, C., Herbert, G., and Hass, W. A. (**1967**). "Meteorological investigations. National Sonic Boom Evaluation Office: Sonic boom experiments at Edwards Air Force Base," Report No. NSBEO-1-67.
Saha, S., Moorthi, S., Wu, X., Wang, J., Nadiga, S., Tripp, P., Behringer, D., Hou, Y.-T., Chuang, H.-Y., Iredell, M., Ek, M., Meng, J., Yang, R., Peña Mendez, M., van den Dool, H., Zhang, Q., Wang, W., Chen, M., and Becker, E. (**2014**). "The NCEP Climate Forecast System, version 2," J. Clim. **27**(6), 2185–2208.
Shepherd, K. P., and Sullivan, B. M. (**1991**). "A loudness calculation procedure applied to shaped sonic booms," Report No. NASA-TP-3134.
Sheskin, D. J. (**2000**). *Handbook of Parametric and Nonparametric Statistical Procedures* (CRC, Boca Raton, FL).
Stevens, S. S., VII (**1972**). "Perceived level of noise by mark and decibels," J. Acoust. Soc. Am. **51**, 575–601.
Stout, T. A. (**2018**). "Simulation of N-Wave and shaped supersonic signature turbulent variations," Ph.D. dissertation, The Pennsylvania State University, University Park, PA.
Stout, T. A., and Sparrow, V. W. (**2018**). "Nonlinear propagation of shaped supersonic signatures through turbulence," Proc. Mtgs. Acoust. **34**, 045011.
Stout, T. A., and Sparrow, V. W. (**2019**). "Three-dimensional simulation of shaped sonic boom signature loudness variations due to atmospheric turbulence," in *25th AIAA/CEAS Aeroacoustics Conference*, Delft, The Netherlands.
Stout, T. A., and Sparrow, V. W. (**2022**). "Atmospheric turbulence effects on shaped and unshaped sonic boom signatures," J. Acoust. Soc. Am. **151**, 3280–3290.
Stout, T. A., Sparrow, V. W., and Blanc-Benon, P. (**2021**). "Evaluation of numerical predictions of sonic boom level variability due to atmospheric turbulence," J. Acoust. Soc. Am. **149**(5), 3250–3260.
Vaisala (**2017**). "Radiosonde RS41-SGP Hardware Specification Sheet" (Vaisala, Vantaa, Finland).
Wilson, D. K. (**2000**). "A turbulence spectral model for sound propagation in the atmosphere that incorporates shear and buoyancy forcings," J. Acoust. Soc. Am. **108**, 2021–2038.

14 September 2026 20:23:01